Ultrafast Structural Dynamics of Photochromic Indolylfulgimides Studied by Vibrational Spectroscopy and DFT Calculations

Florian O. Koller,[†] Wolfgang J. Schreier,[†] Tobias E. Schrader,[†] Arne Sieg,[†] Stephan Malkmus,[†] Christine Schulz,[‡] Steffen Dietrich,[‡] Karola Rück-Braun,[‡] Wolfgang Zinth,[†] and Markus Braun*[,†]

BioMolekulare Optik, Department Physik, Ludwig-Maximilians-Universität München, Oettingenstrasse 67, D-80538 München, Germany, and Institut für Chemie, Technische Universität Berlin, Strasse d. 17. Juni 135, D-10623 Berlin, Germany

Received: September 5, 2006; In Final Form: September 28, 2006

The structural dynamics of the ring-opening reaction in a photochromic indolylfulgimide, a reversible, ultrafast photoswitch, is investigated by ultra-broadband time-resolved vibrational spectroscopy. The experimentally observed vibrational modes of the indolylfulgimide photoisomers *C* and *E* are assigned to normal modes with the help of DFT calculations. A complete evaluation of the observed vibrational dynamics including excited-state vibrational modes is used to characterize the reaction path and the cooling behavior of the photoswitch.

Introduction

Photochromism of molecules is defined as a photoinduced, reversible modification of their chemical structure that induces changes in their absorption spectrum.[1] Isomerization, bond breaking, and bond formation are important reaction types involved in photochromism. In particular indolylfulgides and indolylfulgimides represent an interesting class of photochromic dyes. They exhibit the possibility to design their spectral properties such as addressability in the visible (vis) spectral range, exhibit the thermal stability of their photoisomers, and show high photostability during repeated illumination cycles.[2−6] Fulgides and fulgimides were frequently used to demonstrate optical switching or data storage applications.[4,7−11]

For the investigated indolylfulgimide (see Scheme 1), three photoisomers have to be considered when describing the photoreaction: the ring-closed *C*-form and the ring-opened *E*- and *Z*-forms. Only the *C*-form has a strong vis absorption. The *E*- and *Z*-form can be optically excited only in the UV spectral region. A direct reaction path between the *C*- and the *Z*-form has not been observed.[4] Therefore, the bleaching of the vis absorption band of the *C*-form due to the ring-opening reaction is uniquely addressable and yields the *E*-form as distinct photoproduct accompanied by a strong shift in the optical absorption.

The absorption spectrum of the indolylfulgimide in the UV/vis spectral range consists of few and broad bands containing limited information on the electronic structure of the molecule. In the mid-infrared spectral range (mid-IR) and especially the fingerprint region, more direct information on the conformational structure can be derived. Here, many vibrational modes can be observed in a single experiment and should allow a direct assignment to the photoisomers of the indolylfulgimide. Therefore, photochromism due to a structural change is efficiently analyzed in the mid-IR spectral range. In addition, in the mid-IR the photoisomers can be monitored without inducing photoreaction. As photochromism is a dynamic phenomenon, time-resolved spectroscopy in the mid-IR is a powerful tool for the investigation of the involved dynamics with the high time-resolution required to study these ultrafast photoreactions. Former measurements on indolylfulgimides with probe wavelength in the UV/vis have shown ultrafast kinetics for the ring-opening reaction $C \rightarrow E$ that occurs within about 2 ps.[12]

In this work we present steady-state and time-resolved, broadband mid-IR absorption measurements for the study of the $C \rightarrow E$ ring-opening reaction in the *N*-methylindolylfulgimide under investigation. DFT calculations are employed to assign the observed mid-IR bands to normal modes of the *C*- and *E*-form ground states of the investigated indolylfulgimide. In addition we are able to reveal vibrational modes of the electronic excited state. The complete analysis of the structural sensitive mid-IR spectra offers detailed information on the reaction path and the cooling behavior of the molecule.

Materials and Methods

Sample Preparation. The synthesis of the *N*-methylindolylfulgimide will be published elsewhere. Because of its very low absorbance in the whole mid-IR spectral range, tetrachloroethylene (Sigma-Aldrich, purity 99+%) was used as solvent. The concentration of the *N*-methylindolylfulgimide was about 8 mM in all experiments.

Samples of the pure *C*-form were obtained by purification under exclusion of light via flash-chromatography on silica gel using dichloromethane as eluent and were analyzed by high-pressure liquid chromatography (HPLC). Samples of the pure *E*-form were obtained by vis illumination of the pure *C*-form samples, as the *E*-form is the only photoproduct under these illumination conditions.

Steady-State Experiments. Steady-state absorption spectra in the vis spectral range were recorded with a spectrophotometer (Perkin-Elmer, Lambda19). For the mid-IR absorption and difference spectra, a Fourier transform infrared (FTIR) spec-

* Corresponding author. markus.braun@physik.uni-muenchen.de, Fax: ++49 +89 2180 9202.
[†] Ludwig-Maximilians-Universität München.
[‡] Technische Universität Berlin.

10.1021/jp0657787 CCC: $33.50
Published on Web 11/09/2006

SCHEME 1: Chemical Structures of the Thermally Stable *Z*-, *E*-, and *C*-Forms of the *N*-Methylindolylfulgimide and the Possible Photoreactions That Cause the Photochromic Behavior[a]

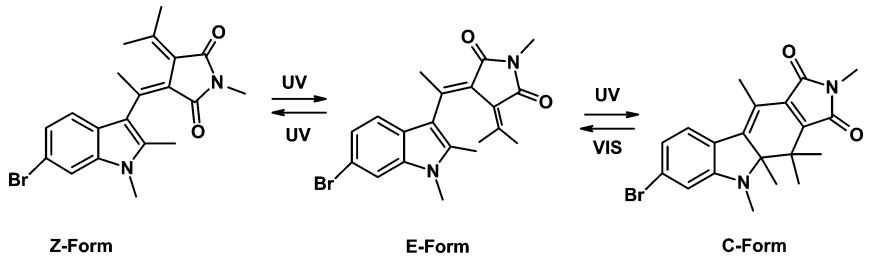

[a] The investigated ring-opening reaction $C \rightarrow E$ is initiated by vis excitation.

trometer (model IFS66 from Bruker) was employed. The samples were measured in cuvettes with CaF_2 windows and an optical path length of about 90 μm. Steady-state conversion from the closed *C*- to the open *E*-form was achieved via vis illumination by a cold light source (KLC2500 from Schott, filtered with color glass filters OG570 and KG2 from ITOS, about 200 mW in the spectral range between 570 and 700 nm). Initiation of the back reaction $E \rightarrow C$ was performed by UV illumination using an Hg(Xe) arc lamp (L.O.T. Oriel, color glass filters WG320 and UG11, about 10 mW at mainly 365 nm). The spot diameter at the sample location was about 15 mm. The duration of UV and vis illumination was 1 min. Photostationary states (PSS: photoisomer mixtures under steady-state illumination with constant concentrations of the *E*-, *Z*-, and *C*-form) were already reached after about 20 s.

The mixture of photoisomers containing the *E*-, *Z*-, and *C*-form obtained after UV illumination (described above) will be referenced as PSS-365. Visible illumination (described above) of the PSS-365 leads to the photoisomer mixture referenced as PSS-550 containing the *E*- and *Z*-form, only. The concentrations of the *Z*-form in the PSS-365 and PSS-550 are identical and around 20% as obtained by ^{1}H NMR and HPLC analysis. During the time-resolved measurements of the $C \rightarrow E$ ring-opening reaction, the PSS-365 was preserved due to the same UV illumination as used for the steady-state experiments.

Time-Resolved Experiments. Femtosecond time-resolved pump−probe experiments (for more details see Schrader et al.[13]) are based on a homemade Ti:sapphire based oscillator-amplifier system (CPA) with a repetition rate of 1000 Hz and pulse durations of 90 fs (fwhm) at 806 nm. For the optical excitation of the $C \rightarrow E$ photoreaction a part of the CPA output was frequency doubled to pump a single-stage noncollinear optical parametric amplifier (NOPA)[14,15] delivering pulses with an energy of 1.0 μJ at 550 nm at the sample location and with a duration of about 55 fs after compression. The pump pulses were focused to a diameter of about 200 μm. The excitation pulses were chopped at 500 Hz.

To generate the tunable mid-IR pulses, multistage parametric processes were used. A tunable OPA pumped with the CPA-output and seeded by a NOPA delivered two near-IR pulses around 1450 and 1830 nm. By difference frequency mixing of these two pulses in an $AgGaS_2$ crystal, the mid-IR pulses were generated with a spectral width of about 150 cm^{-1} (fwhm). The pulse duration of approximately 250 fs was determined by cross-correlation with the pump pulses in germanium. The probe pulses had energies of about 50 nJ and a diameter of 150 μm at the sample position. To cover the whole measured spectral range of 500 cm^{-1}, experiments with three different probe spectra were performed.

At the sample location, the linear polarization of the probe pulse was set to 45° degree with respect to the pump pulse. After passing the sample, the probe pulse was split into two parts using wire grid polarizers. These pulses were polarized parallel and perpendicular with respect to the pump pulses and were recorded in two identical spectrometers (gratings with 100 and 150 lines per mm depending on the probe wavelength) equipped with mercury cadmium telluride (MCT) arrays (32 channels, form Infrared Associates). The resulting spectral resolution was about 3 cm^{-1}. Averaging over 3000 probe pulses resolved absorbance changes down to 50 μOD.

Flow cells with CaF_2 windows (thickness of 2 mm) and a peristaltic pump were used for sample handling; the path length of the sample was 90 μm as in the steady-state experiments. The optical density at the excitation wavelength of 550 nm was about 0.5 OD. The sample was completely exchanged between two consecutive laser shots.

The transient absorption signal of the *N*-methylindolylfulgimide was corrected for the signal component due to the solvent tetrachloroethylene, which was determined separately under identical excitation conditions. Three different mid-IR probe spectra were generated (see above) in order to record the complete data set. The overlap region of the different spectra were at about 1455 and 1640 cm^{-1}. At the wings of the three probe spectra, the noise is increased. The data of the two low-frequency spectra was scaled to match the steady-state difference spectrum.

Calculations. DFT calculations of the *N*-methylindolylfulgimide in a vacuum were carried out using the Gaussian 98[16] program package. The molecular geometry was optimized employing the density functional Becke's three-parameter hybrid method[17,18] using the LYP correlation functional (B3LYP) with the 6-31+G* basis set. Geometries, normal modes, and their amplitudes for the two photoisomers of interest (*C* and *E*) have been calculated. Normal modes and vibrational frequencies were determined at the computed equilibrium geometries by evaluation of the second derivatives of the energy.

Experimental Results

As mentioned above, the *N*-methylindolylfulgimide exists in three thermally stable photoisomers (see Scheme 1). The *Z*-form can photoisomerize (UV excitation) to the *E*-form, only.[4] UV excitation of the *E*-form can yield different reaction pathways: isomerization to the *Z*-form photoproduct or ring-closure reaction to the *C*-form. Visible light (above 450 nm) excites exclusively the ring-closed *C*-form and leads selectively to the *E*-form (ring-opening reaction $C \rightarrow E$). All these photoinduced processes are reversible.[12]

In Figure 1 we present the UV/vis absorption spectra of the pure *C*- and *E*-form (see Materials and Methods). The pronounced vis absorption at 550 nm of the *C*-form and the lack of absorption from the *Z*- and *E*-form in this range allow

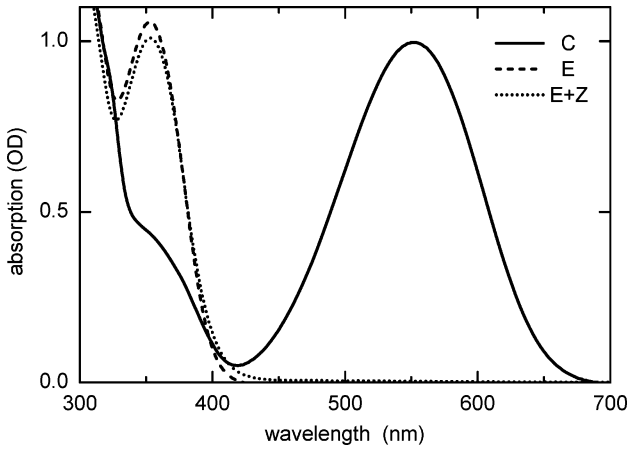

Figure 1. Absorption spectra in the UV/vis spectral range of the pure *C*-form (line), of the pure *E*-form (broken line), and of a photostationary mixture between the *E*- and the *Z*-form (dotted). (For sample preparation, see Materials and Methods).

excitation and monitoring of the $C \rightarrow E$ ring-opening reaction without any involvement of the *Z*-form. The quantum yield for the $C \rightarrow E$ reaction in tetrachloroethylene of about 11% is well in the range reported in the literature for similar compounds.[6]

Also we show the absorption of a typical mixture of *E*- and *Z*-form molecules as obtained in the PSS-550 after several UV and vis illumination cycles. Comparing the spectrum of the pure *E*-form with that of the *E*/*Z* mixture reveals that the UV/ vis absorption spectra of the *E*- and *Z*-form are similar. The fraction of the *Z*-form in a photostationary *E*/*Z* mixture is typically in the range below 20% (as obtained by ^{1}H NMR and HPLC). Nevertheless, the involvement of the *Z*-form in the photoreactions studied in this work can be neglected.

Steady-State FTIR Spectroscopy and DFT Calculations. The $C \rightarrow E$ photoreaction results in a decrease of the absorption band at 550 nm and a corresponding increase of the UV absorption at 360 nm (Figure 1). The mid-IR absorption spectra of the pure photoisomers *C* and *E* show a more detailed picture: in the spectral range between 1300 and 1800 cm^{-1} about a dozen bands are identified that change significantly upon the ring-opening reaction.

Vibrational modes that are appropriate for monitoring the structural dynamics are seen more clearly in the experimental difference spectra (Figure 2d) between the two different photostationary states of the indolylfulgimide PSS-365 and PSS-550. Since the concentrations of the *Z*-form in the sample PSS-365 and PSS-550 are identical, the difference spectra monitor the conversion of the *E*- to the *C*-form by UV illumination (broken line) and the conversion of the *C*- to the *E*-form by vis illumination (solid line). The high symmetry of both difference spectra clearly indicates that the concentration of the *Z*-form is not influenced and that the photoreaction is completely reversible.

A vibrational mode assignment of the strongest mid-IR absorption bands to calculated normal modes is made based on the results of DFT-B3LYP/6-31+G* studies. Hereby, the calculations were performed for the molecule in a vacuum and solute/solvent interactions are neglected. The solvent tetrachloroethylene used in the experiments is nonpolar, weakly interacts with the solute, and shows only very weak IR absorption bands in the spectral range of interest 1300 to 1800 cm^{-1}. Therefore, the employed solvent should not influence the assignment of vibrational modes.

The *N*-methylindolylfulgimide is a polyatomic molecule containing 46 atoms, leading to $3N - 6 = 132$ vibrational

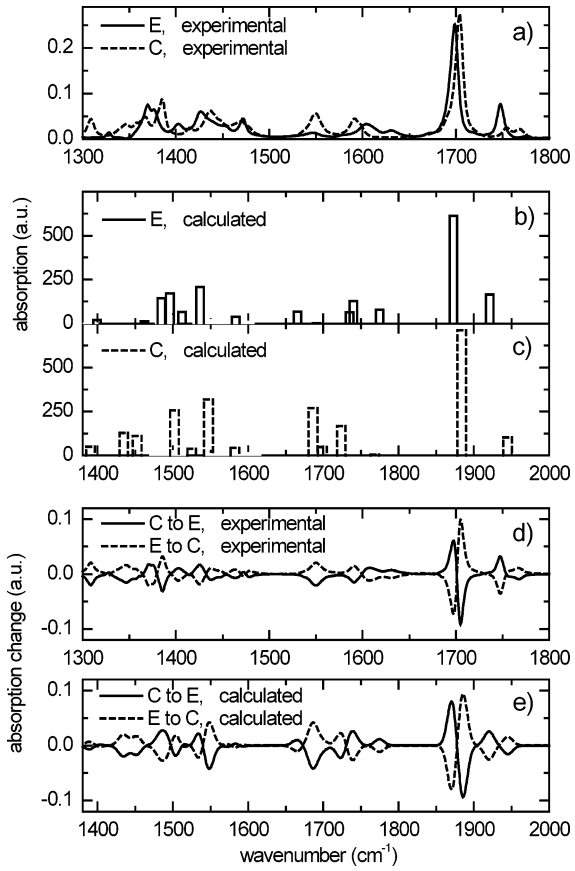

Figure 2. (a) Experimental absorption spectra in the mid-IR spectral range of the pure *E*-form (solid line) and the pure *C*-form (broken line). (b) Normal modes of the *E*-form and (c) *C*-form as obtained from DFT calculation using the correlation functional (B3LYP) with the 6-31+G* basis set. (d) Experimental difference absorption spectra in the mid-IR due to the ring-closure and ring-opening reaction. (e) Difference absorption spectra calculated from the results of the DFT studies (b, c) taking into account the 12 most prominent normal modes. Note the different frequency scale for experimental and theoretical spectra.

TABLE 1: Spectral Positions of the 13 Most Prominent Modes of the *N*-Methylindolylfulgimide in the *C*-Form As Obtained Experimentally by FTIR Absorption Spectroscopy (Figure 2a) and Theoretically by DFT Calculations (Figure 2c)

no.	C^{exp} (cm^{-1})	C^{calc} (cm^{-1})	assignment[a]
C1	1767	1945	ring IV mode; symmetric C=O stretch
C2	1702	1884	ring IV mode; asymmetric C=O stretch
C3	1635	1768	ring III mode; C_1=C_5, C_{15}=C_{16} stretch
C4	1592	1724	ring I mode; C_{10}-H, C_{13}-H bend
C5	1560	1699	ring I and III mode; C_1=C_5, C_{15}=C_{16} stretch
C6	1550	1686	ring I and III mode; C_1=C_5, C_{15}=C_{16} stretch
C7	1471	1582	ring I mode; C_{10}-H, C_{13}-H bend
C8	1437	1547	ring IV mode; N_3-C_2, N_3-C_4 stretch
C9	1413	1525	ring I and II mode; C_{10}-H, C_{12}-H, C_{13}- H bend
C10	1385	1502	ring IV mode; N_3-CH_3 stretch
C11	1365	1452	ring III mode; C_1–C_{16}, C_5-C_6 stretch
C12	1348	1434	ring I and II mode; C_{13}-H bend
C13	1310	1390	ring I and II mode; C_{10}-H, C_{12}-H bend

[a] The assignment is obtained from the theoretical and experimental difference absorption spectra of the strongest vibrational modes (Figure 2d,e).

normal modes. In the spectral range of interest, about 30 normal modes are found in the calculations (Figure 2b,c gives an overview of these modes). The strongest modes (see Tables 1 and 2) are plotted as solid line bars (*E*-form) and broken line bars (*C*-form). The weaker modes, mainly due to methylene

TABLE 2: Spectral Positions of the 14 Most Prominent Modes of the *N*-Methylindolylfulgimide in the *E*-Form

no.	E^{exp} (cm^{-1})	E^{calc} (cm^{-1})	assignment[a]
E1	1747	1921	ring IV mode; symmetric C═O stretch
E2	1695	1873	ring IV mode; asymmetric C═O stretch
E3a	1635	1774	C_5═C_6 stretch
E3b	1603	1740	C_1═C_{16} stretch
E4	1590	1735	ring I mode; C_{10}-H, C_{12}-H, C_{13}-H bend
E5	not obsd	1691	ring I and II mode; C_{12}-H bend
E6	1546	1665	ring I mode; C_7═C_{15} stretch
E7	1473	1583	ring I and II mode; C_{10}-H, C_{13}-H bend
E8	1427	1536	ring IV mode; N_3-C_2, N_3-C_4 stretch
E9	1403	1512	ring II mode
E10	1375	1496	ring IV mode; N_3-CH_3 stretch
E11	1370	1485	ring II mode; N_8-C_7 stretch
E12	1355	1462	ring I and II mode; C_{10}-H, C_{13}-H bend
E13	1330	1399	ring I and II mode; C_{10}-H, C_{12}-H, C_{13}-H bend

[a] The vibrational modes were obtained by FTIR absorption spectroscopy (Figure 2a) and are compared to results of DFT calculations (Figure 2b). Correlation of theoretical and experimental difference absorption spectra (Figure 2d,e) lead to the assignment of vibrational modes.

SCHEME 2: Chemical Structure of the *C*-Form with Atomic Labels as Identification for the Calculated Normal Modes Summarized in Tables 1 and 2

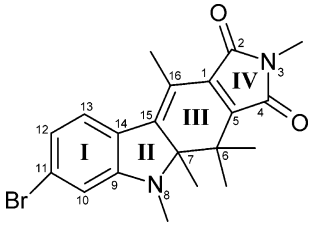

wag vibrations, are plotted in light gray. As expected for such a large molecule, the matching between calculated and experimental spectra is not perfect, especially with respect to the absolute frequencies of the modes (a scaling factor for the frequency was not used here, but note different frequency axes for experimental and calculated spectra),[19] though a first comparison of the experimental and calculated spectra reveals a good agreement, taking into account the 13 strongest modes selected from the calculations for both photoisomers. For Figure 2e, the calculated modes and amplitudes were convoluted with Gaussian line shapes of about 15 cm^{-1} (fwhm). The two generated spectra for the *C*- and *E*-forms were subtracted from each other, and the resulting difference spectra were plotted. Especially for the experimental and calculated difference spectra (Figure 2d,e), good agreement is found that allows for a reliable mode assignment.

We should mention a spectral feature that is not explained with the help of the performed calculations. This is the double-peak shape of the vibrational mode at 1753 and 1767 cm^{-1} for the *C*-form (Figure 2a,c). The band assignment corresponding to the calculations is very explicit in this spectral range, leaving no place for an additional mode. Therefore, one may argue that the observed feature originates from a Fermi resonance.

Tables 1 and 2 together with the Schemes 2 and 3 give an overview of the resulting band assignment. With exception of the spectral region between 1400 and 1475 cm^{-1} where many weakly absorbing modes (mainly CH_3 bending modes) are found, the assignment is obvious.

The ring-opening reaction strongly modifies the molecular structure, and the normal modes described here could be identified in both photoisomers. The experimentally found and calculated frequencies of the normal modes are compared in Table 1 for the *C*-form and Table 2 for the *E*-form of the indolylfulgimide. Atomic motions related to the different vibrational modes are visualized in Scheme 3.

Time-Resolved Measurements. In a previous publication, time-resolved transient absorption data in the UV, vis, and a limited set in the mid-IR were presented[12] and the kinetics of the $C \rightarrow E$ ring-opening reaction was examined. The finding for the *N*-methylindolylfulgimide was that the excited electronic state of the *C*-form decays to a hot *E*-form ground state with a time constant of about 2 ps, the cooling occurs on a time scale of about 16 ps, and the steady-state difference spectrum was reached after at least 80 ps. These observations are confirmed by the transient data presented in this work. In addition, we will focus in the present publication on the dynamics at early times and on the different behavior of special normal modes.

An overview of the data set obtained by transient absorption experiments in the mid-IR is given by transient spectra taken at different delay times. Within the accuracy of the experiment the dynamics observed for parallel and perpendicular probe polarizations are identical. Therefore, we will concentrate in the following on the experimental data set where pump and probe pulses have parallel polarization with respect to each other (Figure 3).

Figure 3a shows that the transient spectrum for the late delay time of 50 ps closely matches the steady-state difference spectrum. This implies that the essential structural changes are completed after about 50 ps.

The transient spectra for early delay times (e.g., for 0.5 ps in Figure 3b) are dominated by a strong, instantaneous absorption decrease of many vibrational bands and by strong bands with induced absorption around 1500, 1630, and 1670 cm^{-1}. The decrease of these absorption bands can be assigned to the disappearance of the ground state of the *C*-form and the induced absorption bands to excited-state vibrational modes.[12] The remaining signal at late times is about 10% of the maximum bleach signal (see Figure 3b). This indicates that about 10% of the excited molecules have acquired a new form. Thus, the transient data confirm the quantum efficiency determined independently by the steady-state measurements (see Materials and Methods).

Figure 4 offers an alternative representation of the data in a 2D plot (positive absorbance changes are red-colored and absorbance decreases are blue-colored). Before and around time-zero, well-known effects such as perturbed free induction decay and cross-phase modulation are observed.[20] For the discussion of structural dynamics, we will use only transient absorption data for delay times longer than 0.5 ps.

The observed signals induced by the excitation pulse can be classified according to their similar temporal behavior into four groups:

Instantaneous bleaching (negative amplitude of the transient absorption signal) recovering on a time-scale of 15 to 20 ps and containing a minor contribution from a fast decay component of about 2 ps. This behavior is experimentally observed for six vibrational modes of the *C*-form ground state at 1767, 1702, 1592, 1550, 1471, 1437, and 1385 cm^{-1} (see Figure 5a,d).

Positive, instantaneous absorbance changes decaying predominantly with a time constant of about 2 ps. This behavior is experimentally observed for the vibrational bands at 1675, 1635, and about 1520 cm^{-1} (see Figure 5c).

Positive, instantaneous absorbance changes staying constant for about 5 ps and decreasing on the 15 to 20 ps time-scale to the offset values found in the steady-state difference spectra.

SCHEME 3: Visualization of the Nuclear Motion in the *N*-Methylindolylfulgimide Due to the Vibrational Normal Modes As Obtained by DFT Calculations for (A) the *C*-Form (C1−C13) and (B) the *E*-Form (E1−E13)[a]

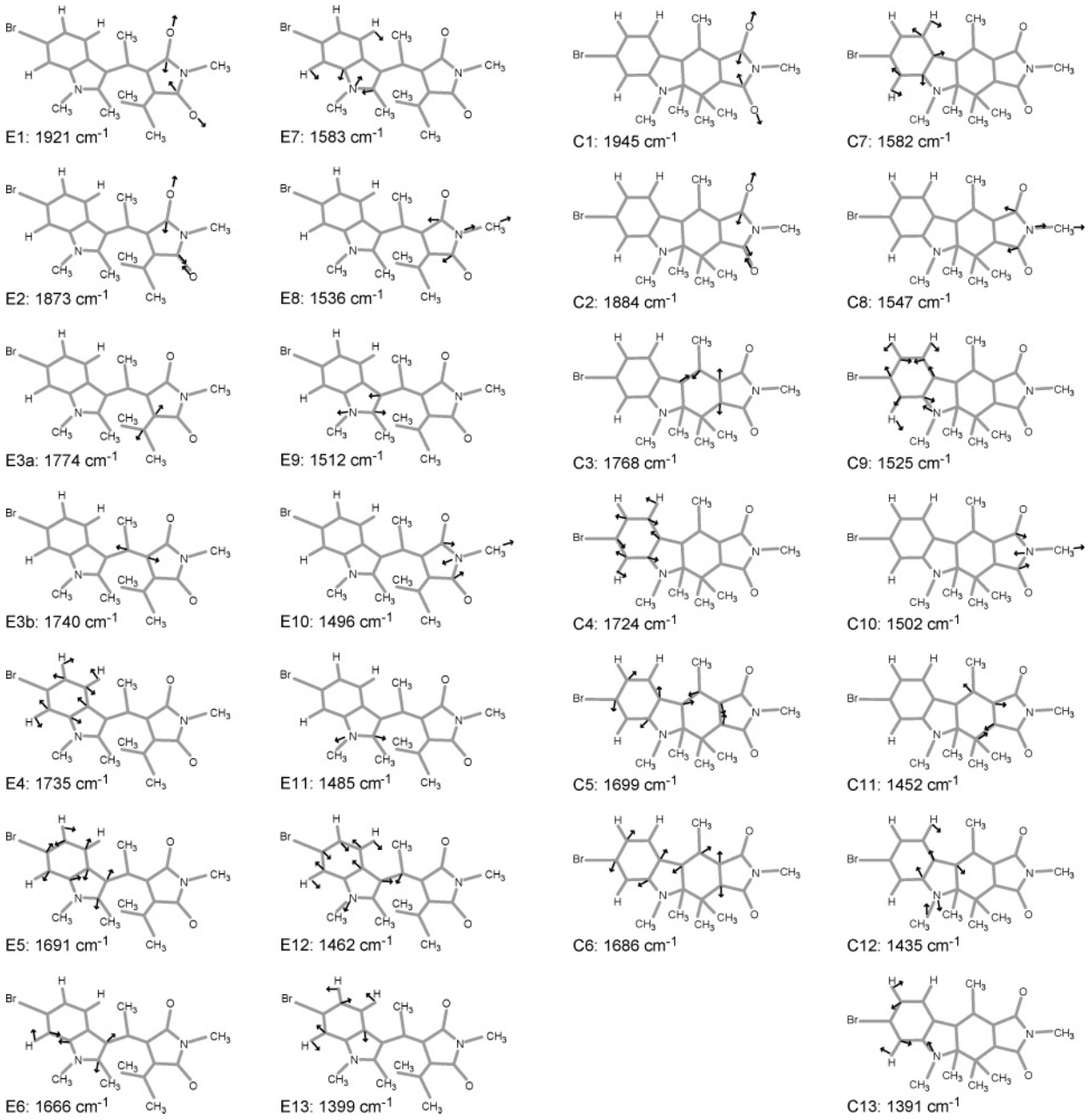

[a] The arrows denote the atomic motion with the strongest amplitude that characterizes the vibrational mode.

This behavior is observed for the bands at 1572, 1403, 1370, 1355, and 1330 cm^{-1} (see Figure 5e).

A delayed rise of a transient absorption with a time constant of about 2 ps combined with a decay with a time constant of about 15 to 20 ps to the offset values found in the steady-state difference spectra. This temporal behavior is found for the vibrational bands at 1747, 1695, 1427, and 1375 cm^{-1} (Figure 5b).

Discussion

For the start of the discussion we will summarize the experimental and theoretical results in brief: the ring-opening reaction induces distinct spectral changes in the mid-IR spectral range. With the help of DFT calculations, the strongest vibrational absorption bands were assigned to normal modes. Time-resolved and steady-state experiments reveal a very good agreement at late delay times, e.g. 50 ps and later. Both the decay of the excited-state absorption and rise of product *E*-form absorption bands occur with a time constant of 2.0 ps. A partial recovery (90%) of the negative bleach signal due to the excited *C*-form occurs within 15 to 20 ps. The remaining amplitudes match the steady-state difference spectrum and are quantitatively in accordance with the observed reaction yield of 10% for the ring-opening reaction. Bands associated with positive absorption changes show different spectral patterns. For an overview of the time-dependent and steady-state behavior of the *N*-methylindolylfulgimide, see Table 3.

Steady-State Spectroscopy and DFT Calculations. The calculated difference spectra (considering the 13 normal modes of Tables 1 and 2) and the experimentally observed difference absorption spectra (see Figure 2) show a very good agreement after some rescaling of the frequency axis. The calculation yields

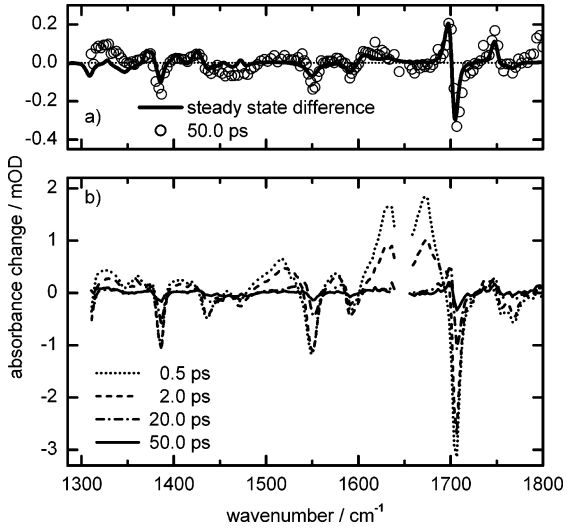

Figure 3. (a) Comparison of the transient absorption spectrum in the mid-IR for a delay time of 50 ps with the steady-state difference absorption spectrum. (b) Transient spectra of the transient absorption data for the delay times 0.5, 2.0, 20 ps, and 50 ps.

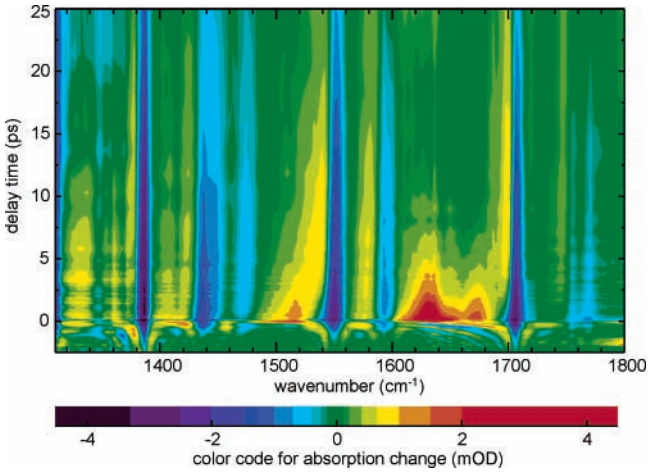

Figure 4. 2D-plot of the time-resolved transient absorption data up to 25 ps. Note the nonlinear color-scaling indicated below. The instantaneous bleach of the vibrational modes due to the *C*-form ground state is observed as a negative signal, color-coded in blue. The instantaneous positive signal due to induced absorption bands of the electronic excited state of the *C*-form is color-coded in red. Before delay time-zero, perturbed free induction decay and cross-phase modulation are observed. The decay of ES absorption and rise of vibrational bands due to the *E*-form photoproduct is seen within the initial 5 ps after photoexcitation.

only very weak IR absorption amplitudes for the other modes in this spectral range. Therefore, the contribution of these modes to the steady-state and transient difference spectra monitoring the ring-opening reaction should be negligible. In the following we will focus on the influence of the photoinduced structural changes on the vibrational modes. (Note, the frequencies given in this section refer to the experimentally observed values).

In the high-frequency range of the measured *C*-form spectrum the symmetric (C1: 1767 cm^{-1}) and antisymmetric (C2: 1702 cm^{-1}) C═O stretch modes are observed. The atomic displacements related to both C═O modes are strongly localized at ring IV (see Scheme 2). This also applies for the symmetric (C8: 1437 cm^{-1}) and antisymmetric (C10: 1385 cm^{-1}) C−N-stretch modes of the imide group. These four strongly localized modes are also found for the molecule in the *E*-form with red-shifted frequencies (E1: 1747 cm^{-1}; E2: 1695 cm^{-1}; E8: 1427 cm^{-1}; E10: 1375 cm^{-1}).

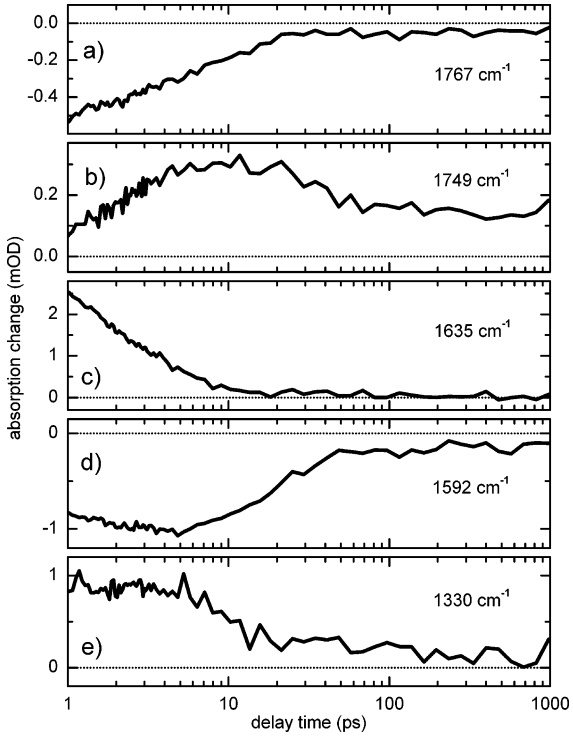

Figure 5. The curves display instantaneous absorption changes and dynamical processes with time constants of 2.0 ps and 15−20 ps. The curves are representative for the grouping of the absorption transients (groups i to iv)).

Normal modes of the *C*-form with nuclear motion distributed over the whole ring system such as the modes C5 and C6 (see Scheme 3a) have no equivalent in the *E*-form. The vibrations in the indolyl group (ring I and II) and in ring IV are found to be completely decoupled from each other when the molecule is in the ring-opened *E*-form (see Scheme 3b).

The vibrational modes C3, C5, C6, and C11 of the *C*-form and E3a, E3b, E5, E6, and E12 of the *E*-form show large amplitude nuclear motion in ring III where the ring-opening occurs. The modes C3, C5, and C6 are found in a frequency range where C═C stretch vibrations are expected. Therefore (see Schemes 2 and 3a), the bonds C_1═C_5 and C_{15}═C_{16} should have strong double bond character. The mode C11 (C_5−C_6 and C_1−C_{16} bond) corresponds to a C−C single bond vibration. For the *E*-form, the modes E3a, E3b, E5, and E6 are in the frequency range for C═C double bond stretch modes, and here the C_5═C_6, C_1═C_{16}, and C_7═C_{15} bonds show large amplitude nuclear motions (see Schemes 2 and 3b). The mode E12 that is in the range of C−C single bond stretch modes has large amplitude motion on the C_{15}−C_{16} bond. This shows that the single and double bond character in ring III is shifted due to the pericyclic ring-opening reaction.

The vibrational modes C4, C7, C9, C12, and C13 in the *C*-form and the matching modes E4, E7, E9, E12, and E13 of the *E*-form can be described by dominant nuclear motion within the indolyl group. For these modes, the vibrational difference absorption spectrum is mainly due to changes in the oscillator strength.

Interpretation of the Transient Absorption Spectra. As pointed out above (see end of Results), the transient absorption signals can be organized according to their temporal behavior into four groups (i to iv):

Group i: The bands showing the described bleaching signals are identified as vibrational modes due to the ground state of the *C*-form of the indolylfulgimide. After optical excitation these

TABLE 3: Frequency Shift and Relative Absorption Change Obtained for the Vibrational Normal Modes of the *C*-Form and *E*-Form in Steady-State Experiments

	steady-state absorpt ion				time-resolved behavior		
no.	*C*, cm^{-1}	*E*, cm^{-1}	Δ, cm^{-1}	Δ_{ampl}	instantaneous	~2 ps	>20 ps
1	1767		−20	+100%	++	+	+
		1747			−	++	+
2	1702		−7	−15%	++	+	+
		1695			−	++	+
3	1635		(0	+ 1000%	covered by excited-state absorption		
		1635 (1603)					
4	1592		−2	−25%	++	+	++
		1590			covered by excited-state absorption		
5	1560		N/a	−95%	N/a		
		Not obsd			N/a		
6	1550		(−4)	(−75%)	++	+	+
		1546			covered by excited-state absorption		
7	1471		+2	(0%	+	+/−	+
		1473			covered by excited-state absorption		
8	1437		−10	−25%	++	−	+
		1427			−	+	+
9	1413		−10	+80%	N/a		
		1403			++	+/−	+
10	1385		−10	−25%	++	−	+
		1375			−	+	++
11	1365		(+5)	(+20%)	N/a		
		1370			++	+/−	+
12	1348		+7	−90%	++	+	++
		1355			++	+/−	+
13	1310		+20	− 70%	N/a		
		1330			++	+/−	+

[a] The temporal behavior (rise and decay characteristics) was determined by fs pump−probe spectroscopy.

bands are bleached instantaneously. The decay of this bleaching signal occurs within 15 to 20 ps, which can be identified as the typical cooling time of the *C*-form ground state[12] due to nonreacting molecules. The recovery of the bleach is observed with an amplitude of about 90%, which fits well to the reaction yield of 10% for the ring-opening reaction.

Groups ii and iii: At early delay times, these signals can be attributed to the instantaneous rise of the absorption due to excited state (ES) vibrational modes of the *C*-form. For the modes of group ii, a decay time of 2 ps is observed, which fits well to the ES lifetime of the indolylfulgimide *C*-form. The modes of group iii are identified as due to the photoproduct ground state (*E*-form). For these modes, the decay of the excited state (time constant of 2 ps) overlaps with the rise of the photoproduct ground state (time constant 2 ps). Therefore, a plateau (for about 5 ps) is observed in the transients for these bands.

Group iv: The delayed rise for the signals of this group has a time constant of about 2 ps. This time constant is identified with the decay time of the electronic ES (*C*-form) and the formation time of the photoproduct (*E*-form) due to the ring-opening reaction. These modes are located in ring IV: both C═O stretch modes at 1747 and 1695 cm^{-1} and both C−N-stretch modes at 1427 and 1375 cm^{-1}. The signal also reflects cooling dynamics with about 15 to 20 ps; for longer delay times, it remains constant. As the spectrum for long delay times matches the steady-state difference spectrum the assignment of the bands in group iv to ground-state modes of the *E*-form is justified.

In conclusion, the steady-state absorption studies, DFT calculations, and transient absorption studies confirm the reaction scheme of the ring-opening reaction as presented in a previous publication.[12] The formation of the photoproduct (*E*-form) and decay of the ES of the educt (*C*-form) are observed with a time constant of 2 ps. The cooling dynamics of the hot nonreacted molecules (*C*-form) and ring-opened molecules (*E*-form) occur in about 15 to 20 ps.

Vibrational cooling is observed for hot modes at 1540, 1580, and 1695 cm^{-1}. They are associated with the bleached bands of the *C*-form ground state at 1550, 1592, and 1702 cm^{-1}. These modes show a spectral blue-shift of about 10 to 15 cm^{-1} on a time scale of 5 to 10 ps. This temporal behavior is significantly slower than the electronic ES lifetime.

It is well-known[13] that due to the off-diagonal anharmonicity of a vibrational mode, induced absorption occurs at the red-wing of a hot absorption band. The amount of this red-shift is a measure for the anharmonicity and the coupling to other, thermally excited (low-frequency) modes. Therefore, the mode at 1550 cm^{-1}, which is seriously influenced by the ring-opening, seems to strongly couple to other low-frequency modes. Also the normal modes at 1592 and 1695 cm^{-1} show anharmonic coupling.

The transient absorption changes yield the following model of the light-induced reaction in the indolylfulgimide. The initially formed excited electronic state decays with a time constant of 2 ps into a ground state product, which shows the signature of vibrationally hot *C*-form with some contributions from the ring-opened *E*-form. On the 15 to 20 ps time scale, cooling of the molecules leads to a different spectrum, which is for delay times greater 50 ps, very similar to the one observed in steady-state illumination experiments. From the remaining bleach of the absorption bands of the *C*-form, one can deduce the quantum efficiency for the ring-opening to be about 10%.

Vibrational Modes in the Excited Electronic State. The ultra-broadband measurements presented here, which cover a spectral range of about 500 cm^{-1}, offer a closer look to the mid-IR spectrum of vibrational modes in the electronic ES. As outlined above, vibrational bands with an instantaneous rise and a fast decay (time constant of about 2 ps) can be attributed to ES absorptions (bands in groups ii and iii). However, because

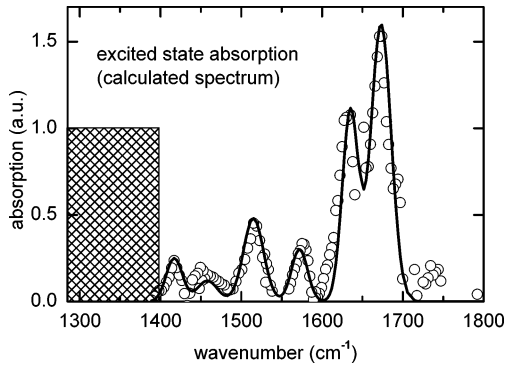

Figure 6. Vibrational spectrum of the *C*-form in the electronic excited state (open circles) obtained as the difference of the transient absorption spectrum at 1.0 ps and the steady-state ground-state absorption of the *C*-form, which accounts for the bleaching features in the transient spectrum. Because of enhanced noise below 1400 cm^{-1}, only vibrational bands with higher frequencies were taken into account. The obtained reproduced ES spectrum was fitted by a set of Gaussians for better representation (solid line).

of the large number of vibrational modes due to the bands of the hot photoproduct and the strong bleaching signal, it is difficult to deduce directly the ES absorption spectrum.

A reconstructed absorption spectrum of the vibrational modes in the electronic excited state is plotted in Figure 6 (dotted line). It is obtained as the difference of the transient absorption spectrum for early delay times (1.0 ps) and the scaled steady-state absorption spectrum of the *C*-form ground state, which resembles the strong bleaching contribution to the signal. As an additional test, it was verified that the transients of the obtained vibrational bands for the ES indeed show positive amplitude for the 2.0 ps decay component.

In the following we will give a tentative assignment of the vibrational bands in the ES of the *C*-form to the corresponding normal modes calculated for the ground state by DFT methods (see above). Three strong ES bands are found at 1515, 1635, and 1673 cm^{-1}. Weaker bands are identified at around 1408, 1458, and 1572 cm^{-1}. As described above the C═O stretch vibrational modes in the 1700 cm^{-1} region of the new-built *E*-isomer rise with the decay-time of the ES. Because of the photoexcitation, the bond character in ring IV changes and the C═O bond is weakened in the electronic ES, which leads to a red-shift of the vibrational C═O modes. So, the two ES vibrational bands at 1635 and 1673 cm^{-1} can be assigned to the C═O stretch modes. The manipulated bond-character of ring IV in the ES influences the C−N modes at 1375 and 1427 cm^{-1} and should shift both to higher frequencies. The two weak ES bands in this spectral region (1408 and 1458 cm^{-1}) would fit to this expected behavior.

According to the assignment of the ground-state bands, the remaining ES absorption bands at 1515 and 1572 cm^{-1} should correspond to large amplitude atomic motion in ring I and ring III, where the ring-opening reaction occurs (see Table 1). The ES mode at 1572 cm^{-1} ought to be associated with the planar ring mode of ring I (mode C4 in Table 1), and the ES mode at 1515 cm^{-1} should be associated with the mode in ring I and III (mode C6 in Table 1), which is mainly due to C═C stretch vibration.

The assignment from above relies only on calculations for the electronic ground state. For a final assignment, the calculations should be performed for the electronic excited state. At present this task is at or beyond the limits of current computational methods. The experimentally determined vibrational spectra of the electronic excited state may serve to verify quantum chemistry calculations of vibrational normal modes in the electronic excited state for a reactive molecule.

Conclusion

In this work we have resolved the structural dynamics connected to the *C* to *E* ring-opening reaction in a molecular photoswitchable indolylfulgimide. The observed dynamics include ultrafast decay of the electronic excited state and photoproduct formation with a time constant of 2.0 ps followed by vibrational cooling on a 15 to 20 ps time scale. Vibrational analysis (DFT calculations) in the electronic ground state leads to an assignment of normal modes for the *E*- and *C*-isomers of the indolylfulgimide. The transient mid-IR data yielded the vibrational spectrum in the electronic excited state. This information could be used in the future for a detailed description of excited-state potential energy surfaces and reaction pathways.

References and Notes

(1) Bouas-Laurent, H.; Dürr, H. *Pure Appl. Chem.* **2001**, *73*, 639−665.
(2) Stobbe, H. *Ber. Dtsch. Chem. Ges.* **1905**, *38*, 3673−3685.
(3) Heller, H. G.; Langan, J. R. *J. Chem. Soc., Perkin Trans. 2* **1981**, 341−343.
(4) Yokoyama, Y. *Chem. Rev.* **2000**, *100*, 1717−1739.
(5) Wolak, M. A.; Gillespie, N. B.; Thomas, C. J.; Birge, R. R.; Lees, W. J. *J. Photochem. Photobiol. A* **2001**, *144*, 83−91.
(6) Wolak, M. A.; Thomas, C. J.; Gillespie, N. B.; Birge, R. R.; Lees, W. J. *J. Org. Chem.* **2003**, *68*, 319−326.
(7) Seibold, M.; Port, H.; Wolf, H. C. *Mol. Cryst. Liq. Cryst. Sci. Technol. Sect. A* **1996**, *283*, 75−80.
(8) Seibold, M.; Port, H. *Chem. Phys. Lett.* **1996**, *252*, 135−140.
(9) Inada, T.; Uchida, S.; Yokoyama, Y. *Chem. Lett.* **1997**, 321−322.
(10) Ramsteiner, I. B.; Hartschuh, A.; Port, H. *Chem. Phys. Lett.* **2001**, *343*, 83−90.
(11) Chen, Y.; Li, T. K.; Fan, M. G.; Mai, X. S.; Zhao, H.; Xu, D. Y. *Mater. Sci. Eng., B* **2005**, *123*, 53−56.
(12) Malkmus, S.; Koller, F. O.; Heinz, B.; Schreier, W. J.; Schrader, T. E.; Zinth, W.; Schulz, C.; Dietrich, S.; Rück-Braun, K.; Braun, M. *Chem. Phys. Lett.* **2006**, *417*, 266−271.
(13) Schrader, T.; Sieg, A.; Koller, F.; Schreier, W.; An, Q.; Zinth, W.; Gilch, P. *Chem. Phys. Lett.* **2004**, *392*, 358−364.
(14) Wilhelm, T.; Piel, J.; Riedle, E. *Opt. Lett.* **1997**, *22*, 1494−1496.
(15) Riedle, E.; Beutter, M.; Lochbrunner, S.; Piel, J.; Schenkl, S.; Spörlein, S.; Zinth, W. *Appl. Phys. B: Laser Opt.* **2000**, *71*, 457−465.
(16) Frisch, M. J.; Trucks, G. W.; Schlegel, H. B.; Scuseria, G. E.; Robb, M. A.; Cheeseman, J. R.; Zakrzewski, V. G.; Montgomery, J. A., Jr.; Stratmann, R. E.; Burant, J. C.; Dapprich, S.; Millam, J. M.; Daniels, A. D.; Kudin, K. N.; Strain, M. C.; Farkas, O.; Tomasi, J.; Barone, V.; Cossi, M.; Cammi, R.; Mennucci, B.; Pomelli, C.; Adamo, C.; Clifford, S.; Ochterski, J.; Petersson, G. A.; Ayala, P. Y.; Cui, Q.; Morokuma, K.; Malick, D. K.; Rabuck, A. D.; Raghavachari, K.; Foresman, J. B.; Cioslowski, J.; Ortiz, J. V.; Stefanov, B. B.; Liu, G.; Liashenko, A.; Piskorz, P.; Komaromi, I.; Gomperts, R.; Martin, R. L.; Fox, D. J.; Keith, T.; Al-Laham, M. A.; Peng, C. Y.; Nanayakkara, A.; Gonzalez, C.; Challacombe, M.; Gill, P. M. W.; Johnson, B. G.; Chen, W.; Wong, M. W.; Andres, J. L.; Head-Gordon, M.; Replogle, E. S.; Pople, J. A. *Gaussian 98*, revision A.7; Gaussian, Inc.: Pittsburgh, PA, 1998.
(17) Becke, A. D. *Phys. Rev. A* **1988**, *38*, 3098−3100.
(18) Becke, A. D. *J. Chem. Phys.* **1993**, *98*, 5648−5652.
(19) Young, D. C. *Computational Chemistry*; Wiley and Sons: New York, 2001.
(20) Hamm, P. *Chem. Phys.* **1995**, *200*, 415−429.